Propeller Performance Relations

Mark Drela

20 April 2016

Nomenclature

T	propeller thrust	ρ	air density
Q	propeller torque	V	velocity ahead of disk (flight speed)
P_{ideal}	ideal disk power	ΔV	propwash velocity increment
P_{shaft}	actual shaft power	V_d	velocity through disk $(= V + \Delta V/2)$
T_c	thrust coefficient based on flight speed	V_e	velocity behind disk $(= V + \Delta V)$
C_T	thrust coefficient based on tip speed	W	velocity relative to blade section
C_P	power coefficient based on tip speed	Δp	pressure jump across disk
β	local geometric blade pitch angle	r	radial coordinate
ϕ	local flow angle	R	propeller tip radius
α	local blade angle of attack $(= \beta - \phi)$	Ω	propeller rotation rate
L'	local blade lift/radius	λ	propeller advance ratio
T'	local blade thrust/radius	η_p	overall propeller efficiency
Q'	local blade torque/radius	η_{ideal}	ideal propeller efficiency

1 Actuator-Disk Model

The simplest model of a propeller is the *Actuator Disk* model, illustrated in Figure 1. The propeller is assumed to be a uniform disk which imparts a static and total pressure increase Δp to any streamline passing through it. The larger total pressure produces an increased "exit" velocity $V_e = V + \Delta V$.

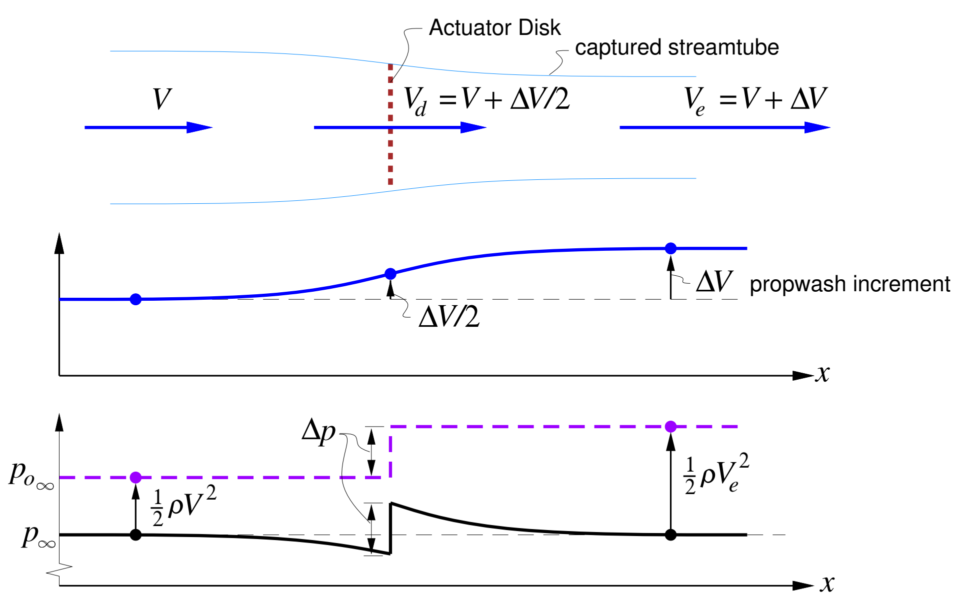

Figure 1: Actuator disk, with velocity, static pressure, and total pressure distributions.

The pressure jump Δp is related to the upstream and exit dynamic pressures through the Bernoulli relation.

$$\begin{aligned} \Delta p &= \tfrac{1}{2}\rho V_e^2 - \tfrac{1}{2}\rho V^2 \\ &= \rho \left(V + \tfrac{1}{2}\Delta V \right) \Delta V \end{aligned} \tag{1}$$

The velocity through the disk is defined as V_d, so that the mass flow through the *captured streamtube* is

$$\dot{m} \;=\; \rho V_d \, \pi R^2 \tag{2}$$

The thrust can be given as the momentum flow increase in the captured streeamtube, and also as the (pressure × area) force on the disk. Equating these two thrust expressions gives

$$\begin{aligned} T \;=\; \dot{m}\,\Delta V \;&=\; \Delta p \, \pi R^2 && (3)\\ \rho V_d \, \pi R^2 \, \Delta V \;&=\; \rho \left(V + \tfrac{1}{2} \Delta V \right) \Delta V \, \pi R^2 \\ V_d \;&=\; V + \tfrac{1}{2} \Delta V && (4) \end{aligned}$$

so that half of the flow acceleration occurs in front of the disk, and the remaining half occurs behind the disk, as shown in Figure 1.

The mass flow through the disk receives an increase in kinetic energy, which must be supplied by the disk at an energy rate (or power) of:

$$\begin{aligned} P_{\text{ideal}} \;&=\; \tfrac{1}{2}\,\dot{m} \left(V_e^2 - V^2 \right) && (5)\\ &=\; \dot{m}\,\Delta V \left(V + \tfrac{1}{2} \Delta V \right) && (6)\\ &=\; T \left(V + \tfrac{1}{2} \Delta V \right) && (7) \end{aligned}$$

This is the minimum power which is required by the disk, dictated by the energy conservation law. The actual power required by a real propeller will be larger because of viscous and other power losses. We now define the *ideal propulsive efficiency*,

$$\frac{TV}{P_{\text{ideal}}} \;\equiv\; \eta_{\text{ideal}} \;=\; \frac{V}{V + \frac{1}{2} \Delta V} \tag{8}$$

which is the maximum attainable efficiency. The actual efficiency will be lower.

To put equation (8) in a more convenient form, we first rewrite the thrust expression (3) and solve it for the *propwash velocity increment* ΔV in terms of the thrust.

$$\begin{aligned} T \;&=\; \rho \left(V + \tfrac{1}{2} \Delta V \right) \Delta V \, \pi R^2 && (9)\\ \Delta V \;&=\; \sqrt{V^2 + \frac{2T}{\rho \pi R^2}} \;-\; V && (10) \end{aligned}$$

Defining a dimensionless velocity-based *thrust coefficient*,

$$T_c \;\equiv\; \frac{T}{\frac{1}{2} \rho V^2 \, \pi R^2} \tag{11}$$

the propwash velocity and ideal efficiency can be concisely given as follows.

$$\begin{aligned} \frac{\Delta V}{V} \;&=\; \sqrt{1 + T_c} - 1 && (12)\\ \eta_{\text{ideal}} \;&=\; \frac{2}{1 + \sqrt{1 + T_c}} && (13) \end{aligned}$$

Figure 2 shows $\Delta V / V$ and η_{ideal} versus T_c. It also shows the captured streamtube shape and streamtubes velocities for light and heavy loading cases, and also for the static-thrust case. The latter has $V = 0$, but a finite $V_e = \Delta V$ as given by equation (10).

$$\Delta V = \sqrt{\frac{2T}{\rho \pi R^2}} \qquad \text{(static thrust case)} \tag{14}$$

$$\eta_{\text{ideal}} = 0 \qquad \text{(static thrust case)} \tag{15}$$

The static case has zero efficiency since it is generating no useful thrust power TV.

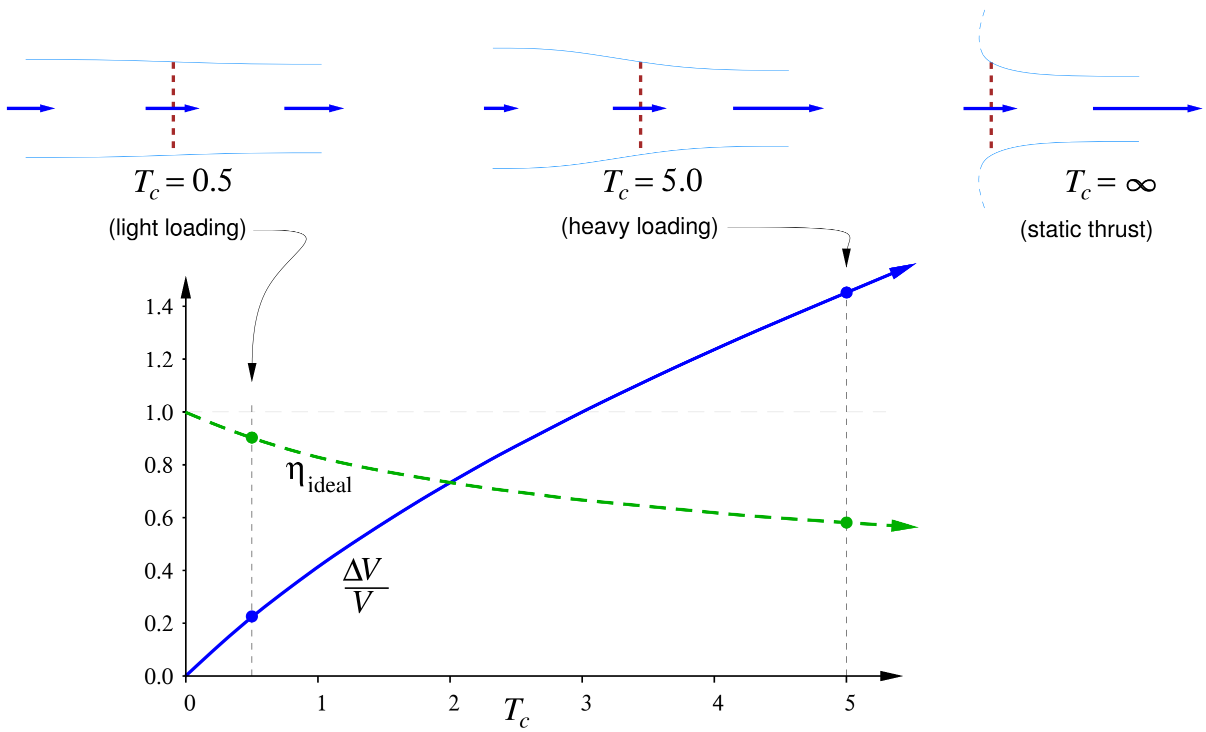

Figure 2: Propwash velocity ratio and ideal efficiency versus thrust coefficient for an actuator disk (ideal propeller). Diagrams at top show different disk loading levels.

The actuator disk relations developed above are applicable to a real propeller, which the actuator disk approximates to a reasonable degree. One limitation is that η_{ideal} is only an upper limit on the efficiency, with the efficiency of an actual propeller being lower by some amount which is not addressed. Another limitation of actuator disk theory is that it gives no insight into how the detailed propeller geometry, other than the tip radius, relates to its aerodynamic behavior. These shortcomings are addressed by the Blade Element Model.

2 Blade-Element Model

The blade element model treats each propeller blade as a wing, which simultaneously translates and rotates in the fluid. Figure 3 shows a propeller blade section at some radius r. The vector combination of the forward flight speed V, the rotational speed Ωr, and the propwash increment $\Delta V/2$ produces the net relative velocity W. This has some angle of attack α relative to the blade airfoil, resulting in section lift/radius and drag/radius forces.

$$L' = \tfrac{1}{2}\rho W^2 \, c \, c_{\ell(\alpha)} \tag{16}$$

$$D' = \tfrac{1}{2}\rho W^2 \, c \, c_{d(\alpha, Re_c)} \tag{17}$$

These forces have a thrust component T' along V, and a torque component Q'/r perpendicular to V which must be balanced by the driveshaft torque.

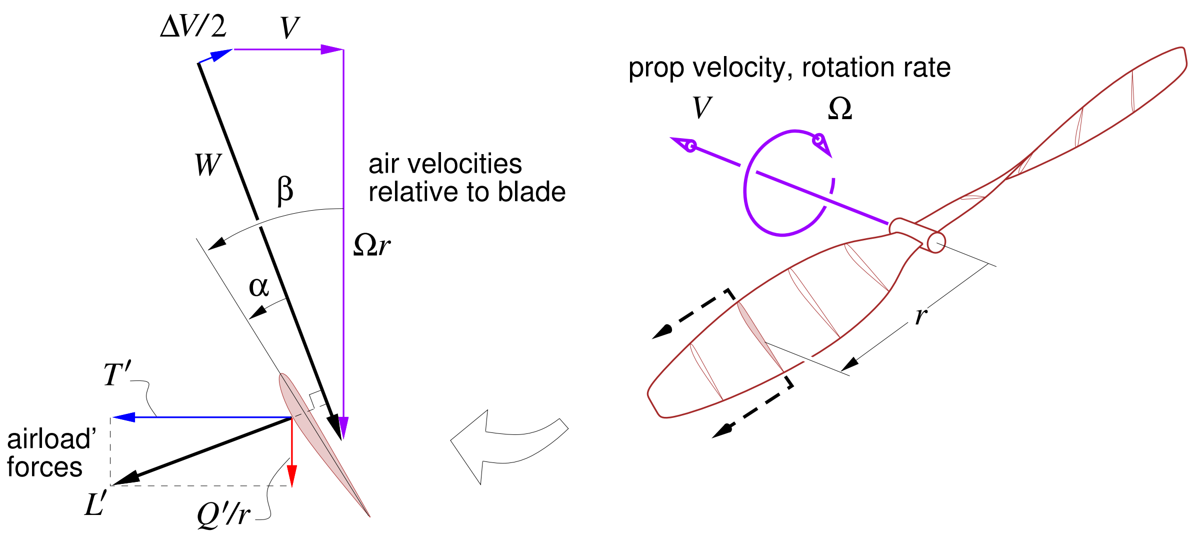

Figure 3: Velocities seen by propeller blade section, producing a blade lift force L' with thrust and torque components. The small profile drag force D' parallel to W is not shown for clarity. This D' will reduce T' and increase Q'/r.

Computation of the overall thrust and torque involves integration of T' and Q' radially along the blade. For a propeller with B blades we then have

$$T = B \int_0^R T' \, \mathrm{d}r \tag{18}$$

$$Q = B \int_0^R (Q'/r)\, r \, \mathrm{d}r \tag{19}$$

Evaluation of these integrals requires detailed knowledge of the propeller geometry, so that α and hence L' can be computed at each radial location. Here we will only consider these forces qualitatively, focusing on how they depend on the propeller operating parameters.

From Figure 3, it is apparent that the local airfoil angle of attack α is the difference between the geometric blade pitch angle β, and the net flow angle ϕ.

$$\alpha = \beta - \phi \tag{20}$$

$$\simeq \beta - \arctan\left[\frac{V + \Delta V/2}{\Omega r}\right] \tag{21}$$

This can be more concisely written in terms of the advance ratio λ as follows.

$$\lambda \equiv \frac{V}{\Omega R} \tag{22}$$

$$\alpha \simeq \beta - \arctan\left[\frac{\lambda}{(r/R)\,\eta_{\text{ideal}}}\right] \tag{23}$$

Therefore, α and the resulting blade lift, thrust, and torque all directly depend on λ. Figure 4 shows a typical blade section on a propeller which is operating at a fixed rotation rate Ω and three forward flight speeds, giving three advance ratios. Clearly, a small λ produces a large α and large aerodynamic loads, and vice versa. The propwash increment $\Delta V/2$ at the propeller tends to partially offset some of this λ influence, so that there is still some relative axial velocity through the disk even in the static case.

The most concise way to describe the aerodynamic behavior of a propeller is via thrust and torque coefficients, much like a wing or airfoil forces are best described by C_L and C_D. However, the

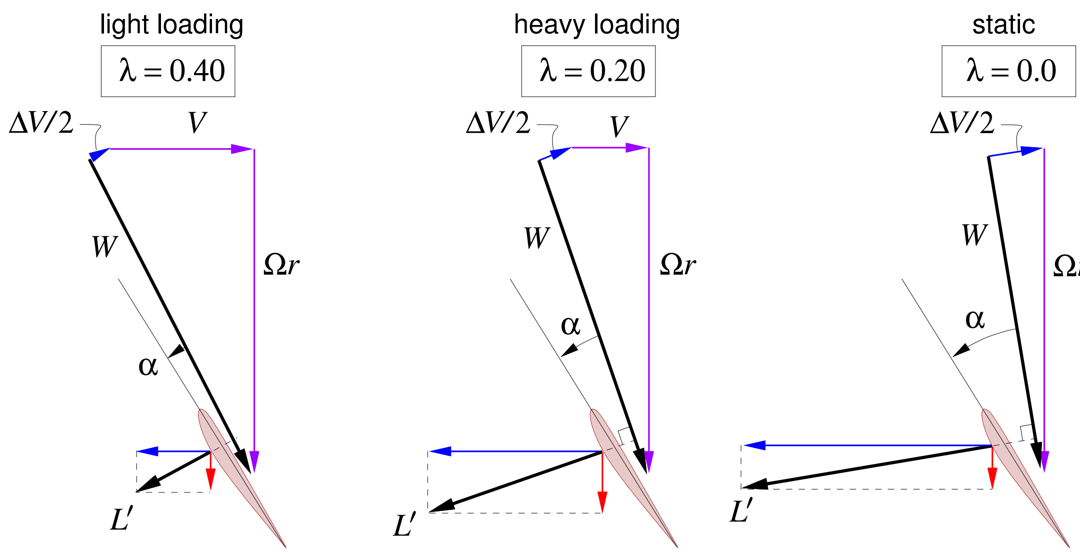

Figure 4: Blade section angle of attack and lift variation with advance ratio.

velocity-based thrust coefficient T_c is not the best choice for this purpose, since $T_c \to \infty$ when $V \to 0$ in the static thrust case. A simple solution to this awkward situation is to use the tip rotational speed ΩR rather than V as the reference velocity. We therefore define the following alternative thrust and torque coefficients.

$$C_T \equiv \frac{T}{\frac{1}{2}\rho(\Omega R)^2\,\pi R^2} \tag{24}$$

$$C_Q \equiv \frac{Q/R}{\frac{1}{2}\rho(\Omega R)^2\,\pi R^2} \tag{25}$$

We can also similarly define a power coefficient which describes the shaft power. But since $P_{\rm shaft} = Q\Omega$, we see that

$$C_P \equiv \frac{P_{\rm shaft}}{\frac{1}{2}\rho(\Omega R)^3\,\pi R^2} = \frac{Q\Omega}{\frac{1}{2}\rho(\Omega R)^3\,\pi R^2} = C_Q \tag{26}$$

so that C_P and C_Q are identical. Note that C_T and T_c are directly related via the advance ratio.

$$C_T = \frac{T}{\frac{1}{2}\rho V^2\,\pi R^2}\,\frac{V^2}{(\Omega R)^2} = T_c\,\lambda^2 \tag{27}$$

Finally, the overall propeller efficiency follows directly from C_T and C_P.

$$\eta_p \equiv \frac{TV}{P_{\rm shaft}} = \frac{C_T\,\lambda}{C_P} \tag{28}$$

Figure 5 shows these parameters versus advance ratio for one particular propeller. It also identifies the points corresponding to the three loading cases in Figure 4.

3 Performance Parameterization

It's important to point out that the curves in Figure 5 are not universal functions of λ, but will also depend on the propeller geometry as characterized by

- pitch/diameter ratio (related to the blade angle $\beta(r)$ distribution)

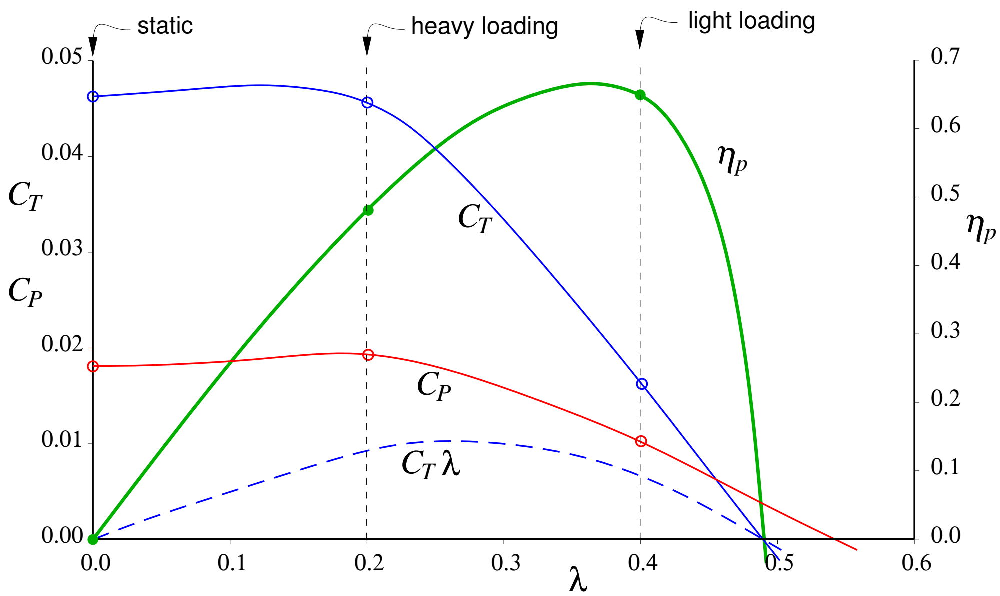

Figure 5: Thrust and power coefficients and efficiency versus advance ratio. The efficiency η_p is the ratio $C_T\lambda/C_P$.

- blade planform (or blade chord $c(r)$ distribution)
- airfoil shape along the blade.

They will also to some extent depend on the average blade-chord Reynolds number, and on the tip Mach number, the latter being defined as

$$M_{\text{tip}} \;=\; \frac{\sqrt{V^2 + (\Omega R)^2}}{a} \;=\; \frac{V}{a}\sqrt{1 + \frac{1}{\lambda^2}} \;=\; M\sqrt{1 + \frac{1}{\lambda^2}}$$

In summary, the parameters have the following dependencies.

$$C_T(\lambda, \text{geometry}, Re, M) \quad , \quad C_P(\lambda, \text{geometry}, Re, M) \quad , \quad \eta_p(\lambda, \text{geometry}, Re, M)$$

For low-speed propellers the Mach number has very little influence, and the Reynolds number often has a weak influence as well. In this case the dependencies simplify as follows:

$$C_T(\lambda, \text{geometry}) \quad , \quad C_P(\lambda, \text{geometry}) \quad , \quad \eta_p(\lambda, \text{geometry})$$

Therefore, the performance of a given low-speed prop is summarized entirely by the three $C_T(\lambda)$, $C_P(\lambda)$, $\eta_p(\lambda)$, curves, shown in Figure 5 as one example.

4 Propeller Pitch Relations

The *local pitch* at a particular radial location is defined as the distance that blade airfoil section would travel in one revolution if it was lined up with the relative oncoming flow. We can line up either the airfoil's chord line, or its zero-lift line, giving two alternative definitions of local pitch,

$$\mathrm{P}_{\text{geom}}(r) \;=\; 2\pi r \,\tan\beta(r) \tag{29}$$

$$\mathrm{P}_{\text{aero}}(r) \;=\; 2\pi r \,\tan\left[\beta(r) - \alpha_{L=0}(r)\right] \tag{30}$$

which are illustrated in Figure 6. The conventional meaning of "pitch" usually refers to P_{geom}, although P_{aero}, is most significant for determining performance characteristics. Note that for a typical cambered propeller blade airfoil, $\alpha_{L=0} < 0$, so that $\mathrm{P}_{\text{aero}} > \mathrm{P}_{\text{geom}}$ as shown in Figure 6.

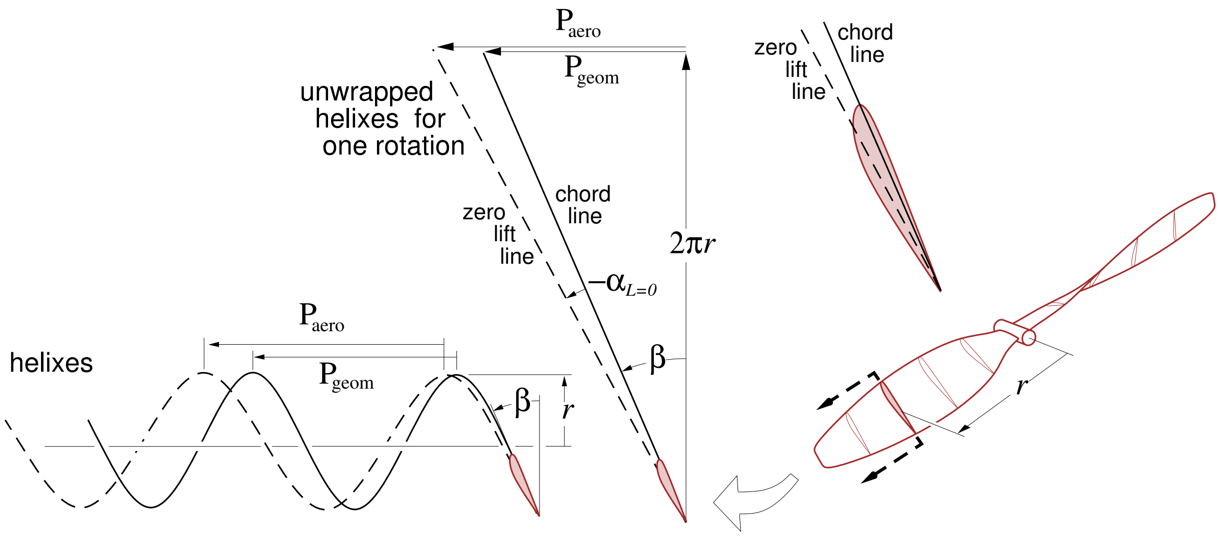

Figure 6: Local pitch relations at one radial r location.

An efficient propeller blade is twisted, as indicated on the right sketch in Figure 6, such that $\mathrm{P}_{\mathrm{geom}}(r)$ or $\mathrm{P}_{\mathrm{aero}}(r)$ do not vary appreciably over the radius. Therefore it's traditional for manufacturers to assign one unique "prop pitch" value P to the whole propeller. One convenient definition is via the blade angle β measured at some representative location, such as 70% radius.

$$\mathrm{P} \;\equiv\; \mathrm{P}_{\mathrm{geom}}(0.7R) \;=\; 2\pi \times 0.7R \times \tan\beta_{0.7}$$

However, this definition is not standard, so two propellers of the same diameter and pitch but different brand name might behave quite differently.

5 Off-Design Operation

For a given aircraft, the propeller is ideally operated close to its best advance ratio, e.g. close to the peak in the efficiency curve $\eta_p(\lambda)$ sketched in Figure 5. This implies that the rotation rate is ideally proportional to airspeed, $\Omega \sim V$. However, most powerplants operate best over a narrower range of rotation rates. If Ω is nearly fixed by the powerplant, we have $\lambda \sim V$, and hence the advance ratio necessarily must vary considerably across the aircraft's velocity range.

For evaluation of such off-design behavior, a useful qualitative parameter is the *pitch/diameter ratio*, or P/D. This indicates how loose or how tight is the helical path that the propeller must take to line up its airfoils with the flow, as shown in Figure 7. A small P/D will typically give good performance at low airspeeds, or low advance ratio λ to be more precise, including the static case $\lambda = 0$. As λ is increased close to the geometric advance ratio $(\mathrm{P/D})/\pi$, the blade angles of attack will decrease to zero and the propeller will "run out of thrust". Further increases in λ will result in windmilling, with negative thrust or braking. Conversely, a propeller with a large P/D will perform poorly at low advance ratios because the resulting large blade angles of attack will result in blade stall. However, such a propeller will become efficient at relatively high advance ratios. From an aircraft operation viewpoint, a smaller P/D favors lower flight speeds, and vice versa. The most common way to accomodate these competing requirements is to use a variable-pitch propeller. This shifts the parameter curves versus advance ratio, as indicated in Figure 8. Both the engine and the propeller can then operate close to their ideal rotation rates across a wide range of aircraft speed.

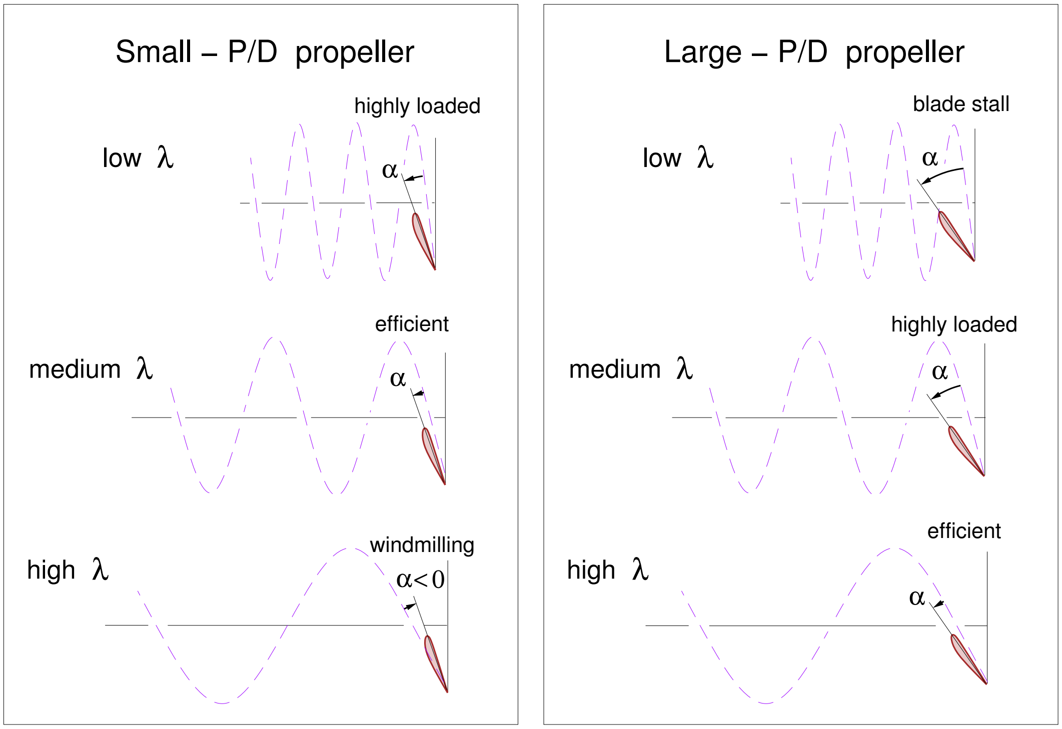

Figure 7: Fixed-pitch propellers with small and large pitch/diameter ratios operating over a range of advance ratios.

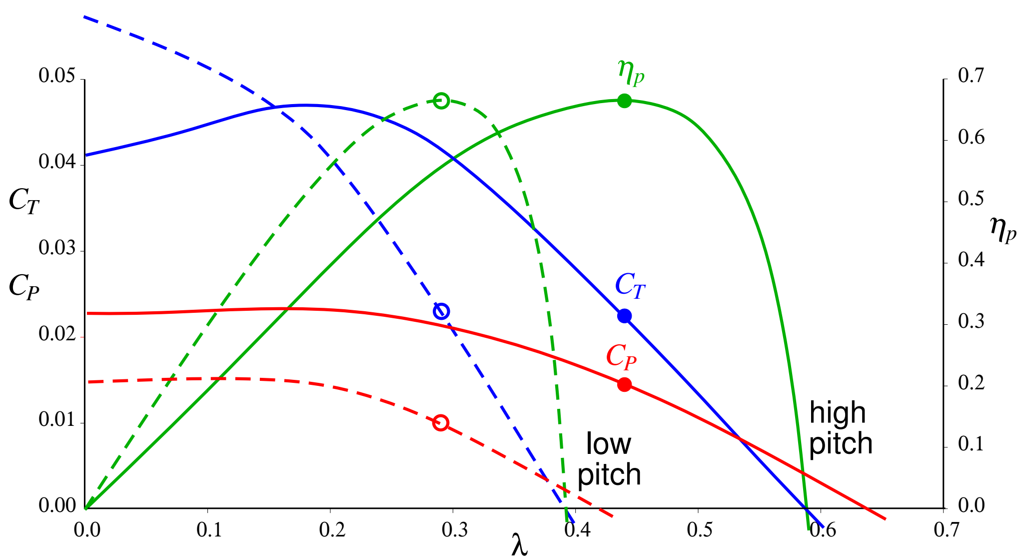

Figure 8: Thrust and power coefficients and efficiency versus advance ratio, for two pitch settings of a variable-pitch propeller. Symbols indicate parameter values at the ideal advance ratio for each pitch setting.